Finite difference acoustic seismic modelling of the iron ore deposit N4WS in Carajás mineral province

Rafael Mansano Holanda*, UFPA and João Carlos Ribeiro Cruz, UFPA

Abstract

This work consists to perform a seismic modeling along a profile in the iron ore deposit of N4WS, situated in the Carajás mineral province. The software Seismic Unix created the geophysical model, which consists of simulating a preliminary geologic model of the iron ore deposit. To create the seismograms and snapshots was used the finite difference program FDSKALAR (SANDMEIER, LIEBHARDT, 1992).

Introduction

The iron ore body N4WS (Figure 1) belongs to the Carajás mineral province and is located in the municipality of Parauapebas, in the southeastern portion of Pará state, within the limits of the Carajás national forest.

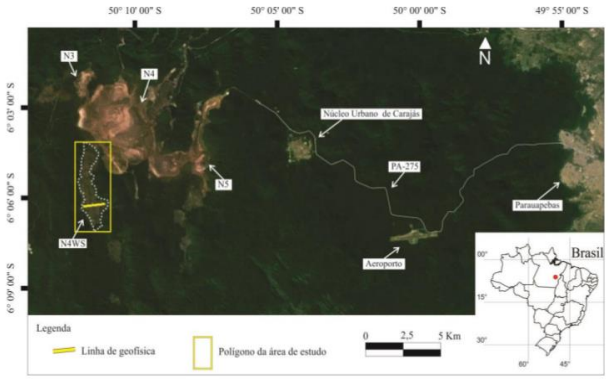

Figure 1 - Location of the study area in N4WS body. Mineral Complex of Carajás, Pará (from Google Earth).

The Carajás mineral province belongs to the Central Amazonian province and is contained in the Amazon Craton (ALMEIDA, HASUI, BRITO NEVES, 1976). It was formed and stabilized during the Archean, subsequently affected by extensive magmatism of Paleoproterozoic age. This province is divided into two tectonic domains, one called granite greenstone terrain Rio Maria, occurring south, Mesoarqueana age, and the other called the Carajás Domain, or Belt Shearing Itacaiúnas, occurring north. The lithostratigraphic unit more prominent in the Carajás mineral province is the Grão-Pará Group, by deposits and mineral occurrences. This unit contains, in deposition order: Parauapebas Formation, Carajás Formation, Igarapé Cigarra Formation and Igarapé Boa Sorte Formation (ARAÚJO, MAIA, 1991). Among these formations, the Carajás Formation stands out because contain bodies of jaspilite and iron ore (MACAMBIRA, 2003; ZUCHETTI, 2007) (Figure 2).

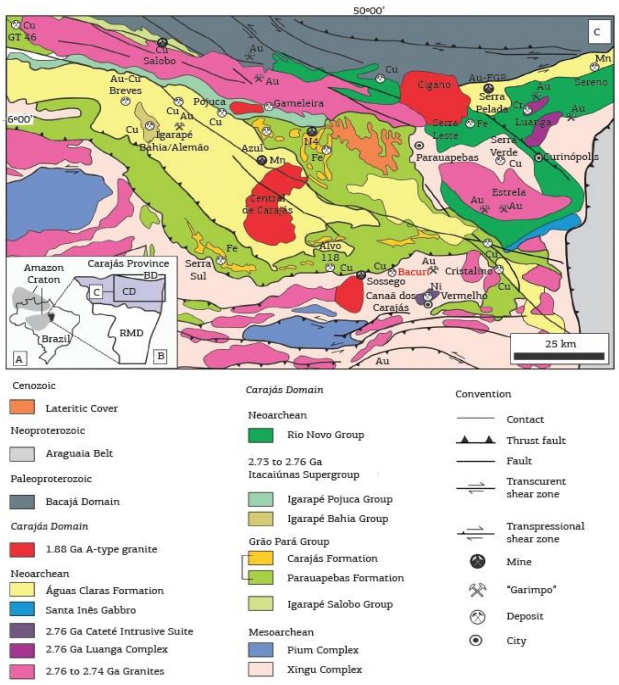

Figure 2 - Geological Map of the Carajás mineral province (modified from Vasquez et al., 2008).

Among the work carried out in the N4WS body, a geological model was built by Nogueira (2014) from the integration of the results obtained by the seismic, electrical resistivity and the aid of 14 drill holes (Figure 3), made by the company Vale S.A. from the data acquisition profile (Figure 4).

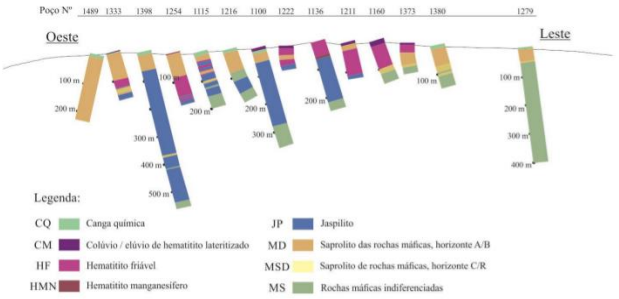

Figure 3 - Profiles drill holes in geophysical lines (seismic refraction and electrical resistivity) with the description of the main lithologies found (from Nogueira, 2014).

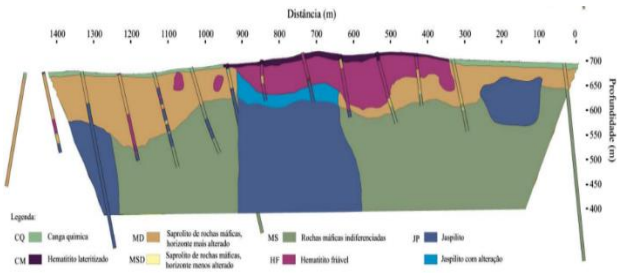

Figure 4 - Interpretative geological model integrating results of seismic refraction and electrical resistivity (from Nogueira, 2014).

This work aims to build a synthetic seismic dataset along a profile on the iron ore deposit of N4WS, from the geological model constructed by Nogueira (2014). We used the finite difference program FDSKALAR to create the seismograms and snapshots (SANDMEIER, LIEBHARDT, 1992).

Methodology

To perform the seismic modeling, we used a finite difference program in Fortran 77 named FDSKALAR developed by Sandmeier and Liebhardt (1992) in the Karlsruhe Universty, Germany. The program is responsible for generating a synthetic seismogram and snapshots by solution of the two-dimensional acoustic wave equation, given by (REYNOLDS, 1978):

$$\frac{1}{c}\frac{\partial^2 u}{\partial t^2} = \frac{\partial^2 u}{\partial x^2} + \frac{\partial^2 u}{\partial z^2}, \qquad (1)$$

where *u* is the pressure of the acoustic wave field, *x* and *z* are cartesian coordinates, *t* is the time and *c* is the velocity of the acoustic wave.

The fourth order approximation to the time and space of finite difference calculates the pressure field. A spatial grid digitizes the two-dimensional model used to simulate the propagation medium (ALFORD, KELLY, BOORE, 1974).

The solution of the wave equation by finite difference operator is a stable process within certain limits. Therefore, it is appropriate to seek the best spacing for the construction of the mesh. According to Holberg (1987), the relationship between the signal dispersion and the mesh opening is given by:

$$\Delta h \leq \frac{\lambda}{8}, \Delta t \leq \frac{\Delta h}{h\sqrt{2}v_{max}}, \qquad (2)$$

where *Δt* is the sampling interval in time; *Δh* is the sampling interval in space; *h* is the factor related to the order of the finite difference operator; *f=1/τ*, $\lambda = v_{min}/f$, v_{min} and v_{max} represent the dominant frequency of the source, the shorter wavelength observed, minimum and maximum velocities assumed in the model, respectively.

Due to the limited memory of computers, the finite difference method obtain the solution for a finite number of points by introducing boundaries that causes reflections. To attenuate these effects, was used the absorbing boundary conditions of Reynolds (1978).

The source used in the algorithm is line source, which has the following numerical notation, according to Sandmeier and Liebhardt (1992):

$$S^n(i,j) = S(x = i\Delta x, z = j\Delta z, t = n\Delta t). \qquad (3)$$

The signal used was the Fuchs-Mueller function mixed phase. According to Sandmeier and Liebhardt (1992), it is represented by:

$$S(n\Delta t) = 4\pi x^2 \left[sen\left(\frac{2\pi n\Delta t}{\tau}\right) - \frac{1}{2}sen\left(\frac{4\pi n\Delta t}{\tau}\right)\right], \qquad (4)$$

where *Δt* is the sampling interval in time, *n* is the spatial sampling index, τ is the signal duration and *x* is the spatial sampling interval.

Results

Based on surveys and seismic refraction performed by Nogueira (2014), velocities of propagation of seismic waves were considered for the lithotype identified during the data acquisition profile (Table 1). From these velocity values, we created a synthetic model that simulates the geological model constructed by Nogueira (2014), using the open source package Seismic Unix software (Figure 5).

Table 1 - Velocity suggested for each lithotype (modified from Nogueira, 2014).

Lithotype	Velocity (m/s)
Chemical canga	1858
Colluvium / alluvium of the altered hematite	
Friable hematite	
Saprolite of mafic rocks, horizon more altered	
Saprolite of mafic rocks, horizon less altered	
Undifferentiated mafic rocks	5413
Jaspilite	

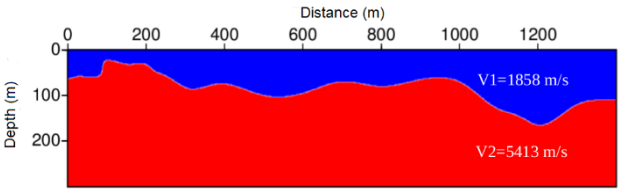

Figure 5 - Synthetic geophysical model created in Seismic Unix package.

For the implementation of FDSKALAR program and creation of synthetic seismograms and snapshots, we used an acquisition geometry based on the data collection scheme carried out by Nogueira (2014) (Table 2).

Table 2 - Acquisition geometry.

Number of points in X direction	560
Number of points in Z direction	120
Sampling interval in seconds	0.0002309
Maximum time in seconds	0.3
Spatial increment of grid in meters	2.5
Number of receivers	250
Distance between receivers in meters	5
Depth of receivers	0
Receiver locations in meters	50 - 1295
Source type	Line source
Source frequency	80 Hz
Length of source signal in seconds	0.0125
Distance between sources in meters	10
Signal type	Fuchs – Mueller
Depth of sources	0
Source locations in meters	100 - 1190
Number of samples for traces on the surface	1299

For better visualization and representation of events in the seismogram, we apply an Automatic Gain Control (AGC). We perform the first shots through the shallower area of the model, where the layer that represent the altered rocks is less thick (Figure 6, 7, 8, 9).

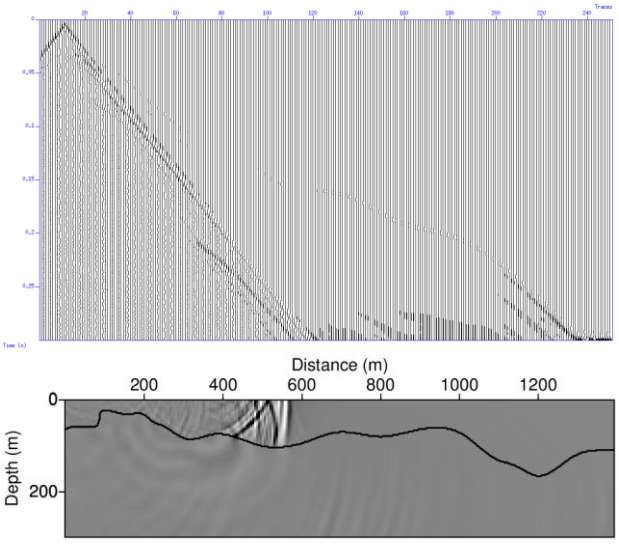

Figure 6 - Synthetic seismogram and snapshot corresponding to the first shot.

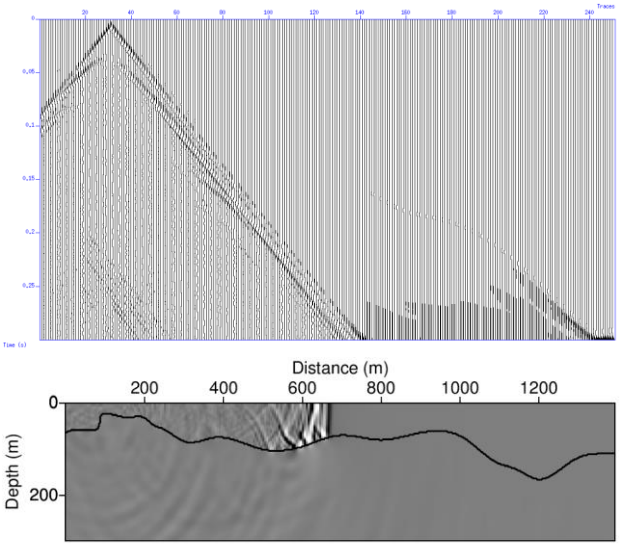

Figure 7 - Synthetic seismogram and snapshot corresponding to the eleventh shot.

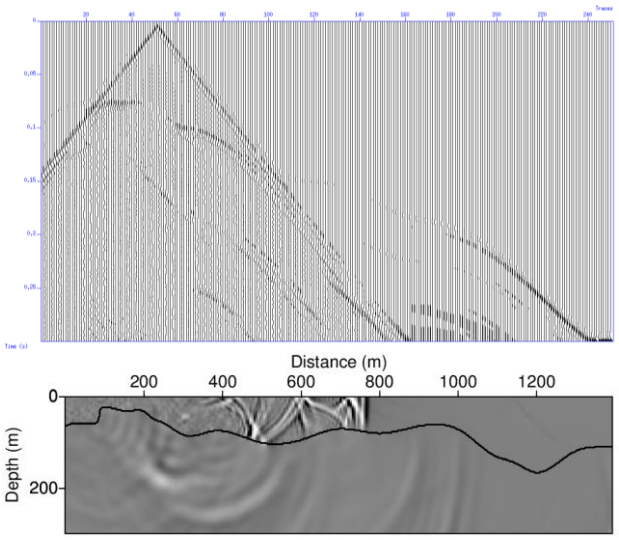

Figure 8 - Synthetic seismogram and snapshot corresponding to the twenty-first shot.

The seismograms and snapshots displays several events associated to diffraction caused by irregularities of the interface. There are also the occurrence of various events associated with reflection, refraction and multiple reflections.

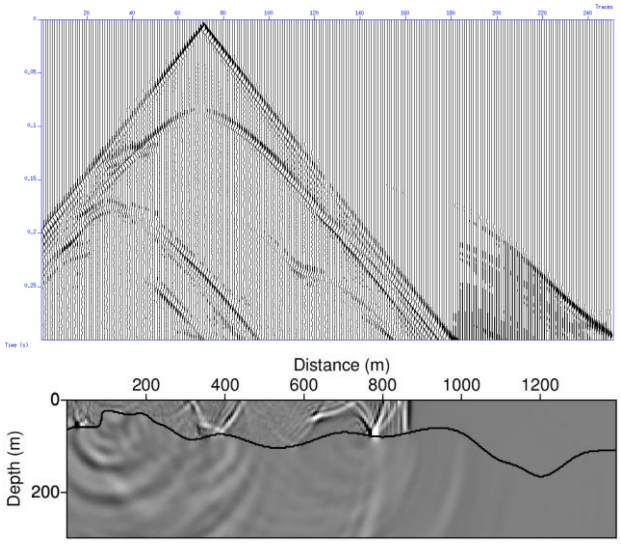

Figure 9 - Synthetic seismogram and snapshot corresponding to the thirty-first shot.

In Figs. 10, 11, 12, 13, 14, 15, 16 and 17, there are the increases of the occurrences of diffraction and "head waves", because the interface continues to show irregularities and by the abrupt change of velocity present in the model. We observe all of them in the seismograph. Such events are also visible in snapshots that displays the various stages of wave propagation.

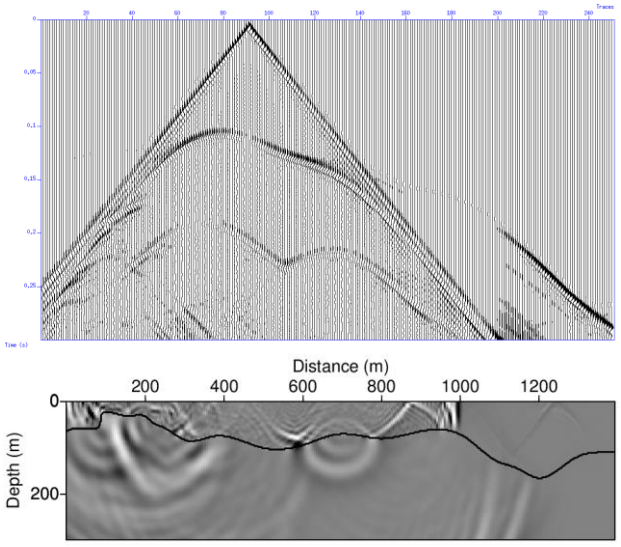

Figure 10 - Synthetic seismogram and snapshot corresponding to the forty-first shot.

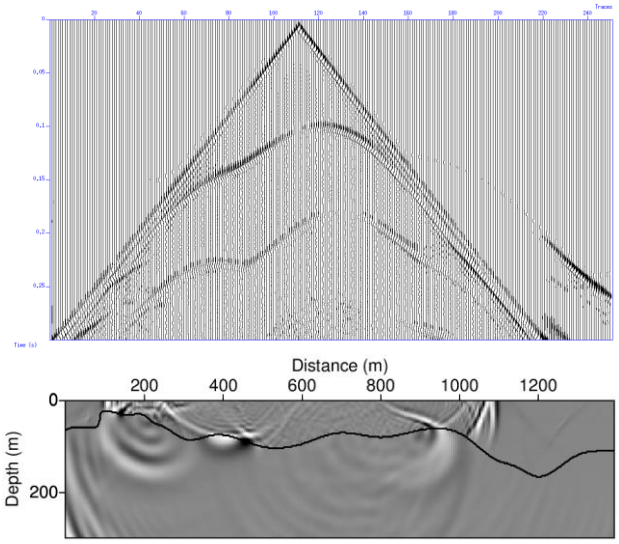

Figure 11 - Synthetic seismogram and snapshot corresponding to the fifty-first shot.

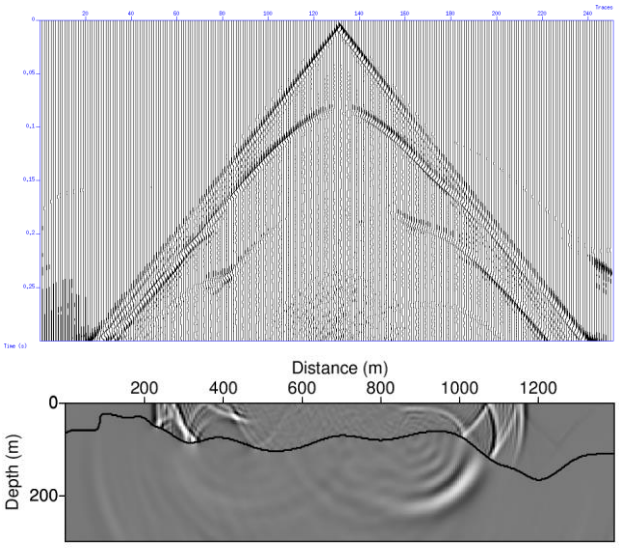

Figure 12 - Synthetic seismogram and snapshot corresponding to the sixty-first shot.

The second model layer representing the preserved rocks, which suffered little influence of weathering, contains high velocity and has great influence on the response of the subsurface to the propagation of seismic waves. Such influence is observed by high amplitudes of the events that are generated at the interface of this layer.

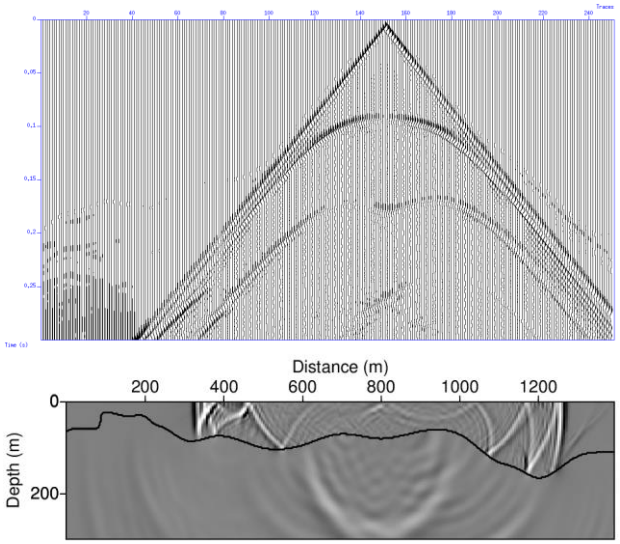

Figure 13 - Synthetic seismogram and snapshot corresponding to the seventy-first shot.

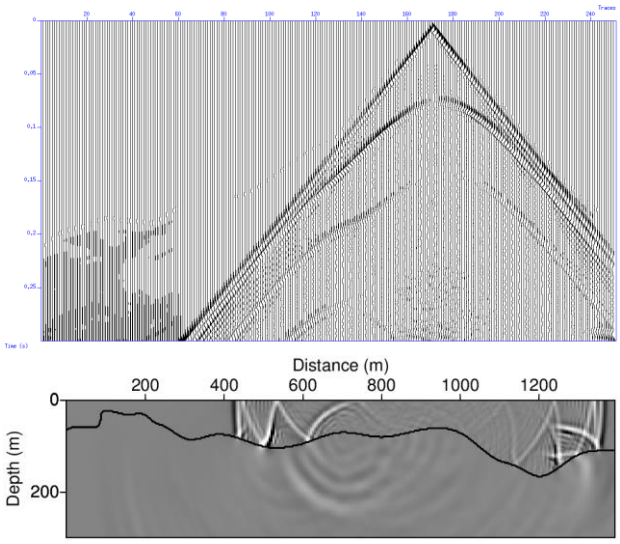

Figure 14 - Synthetic seismogram and snapshot corresponding to the eigthty-first shot.

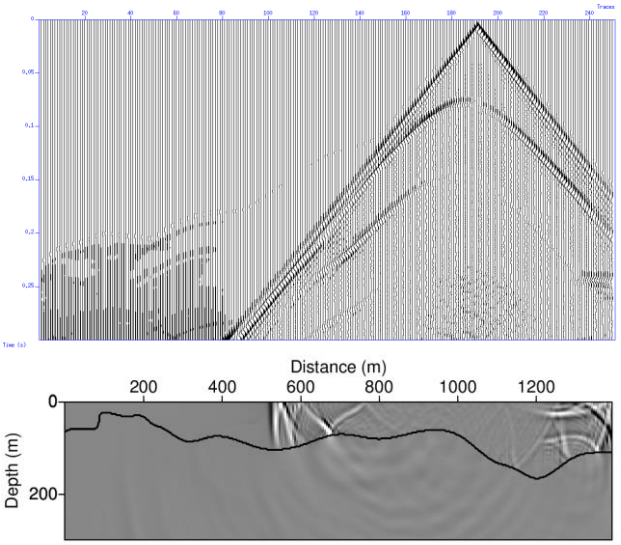

Figure 15 - Synthetic seismogram and snapshot corresponding to the ninety-one shot.

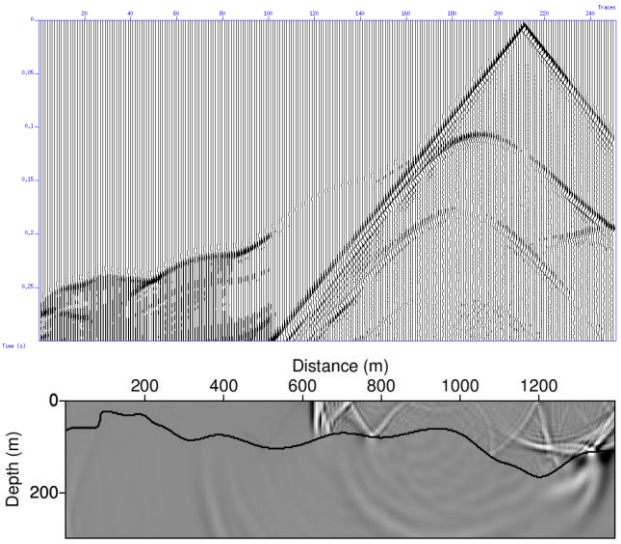

Figure 16 - Synthetic seismogram and snapshot corresponding to the one hundred and one shot.

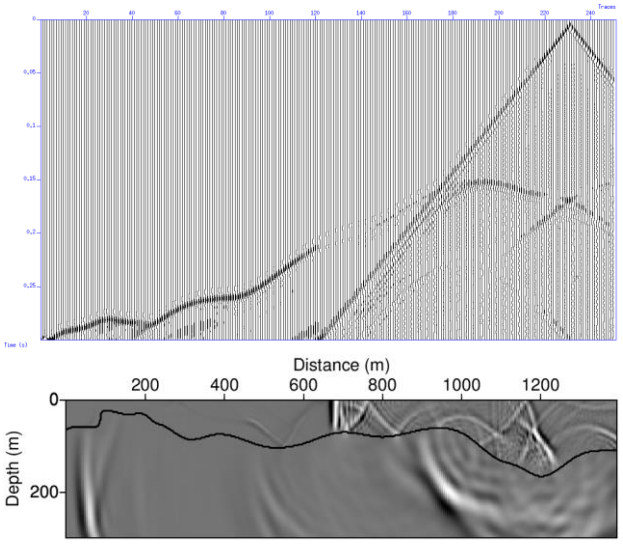

Figure 17 - Synthetic seismogram and snapshot corresponding to the one hundred and eleven shot.

Conclusions

The simulation by the finite difference method is carried out for a finite number of points and by introducing boundaries due to limitation of the computer memory. To select the minimum number of points of the matrix used and the number of steps in time is taken into account evaluation of numerical dispersion, stability and the introduction of absorbing conditions to mitigate any boundary reflections. For these factors, the majority of numerical studies involve problems with dimensional variations of the wave propagation velocity in two spatial dimensions.

The synthetic model used in the present work contains two layers with different velocities (1858 m/s and 5413 m/s) where each layer has been interpreted in terms of the degree of alteration. The first layer groups represents the weathering lithologies (low velocity layer) and second groups preserved lithologies (high velocity layer).

Seismograms and snapshots found the presence of events such as diffraction, reflections, "head waves" and multiple reflections, because the model present irregularities in its interface, with abrupt velocity variation caused by high velocity layer consisting of undifferentiated mafic rocks and jaspilite. The presence of these events may complicate the interpretation of seismic data, being necessary to perform special seismic processing steps, in order to produce acoustic images that allow a better analysis of the results. For obtaining better results in the acquisition data, it is important to use a more sophisticated controlled source, e.g. mini-vibroseis.

Acknowledgements

This work was supported by UFPA and CNPq. Thank the CPGF for the assistance and offered space to perform the work.

References

Alford, R. M., Kelly, K. R. & Boore, D. M., 1974. Accuracy of Finite-difference Modeling of the Acoustic Wave Equation. Geophysics, 39: 834-842.

Almeida, F. F., Hasui Y. & Brito Neves B. B., 1976. The Upper Precambrian of South América. Boletim do Instituto de Geociências, Universidade de São Paulo, São Paulo, Brazil, vol. 7: 45-80.

Araujo, O. J. B. & Maia R. G. N., 1991. Programa levantamentos geológicos básicos do Brasil: Projeto especial mapas de recursos minerais, de solos e de vegetação para a área do Programa Grande Carajás, in: Subprojeto Recursos Minerais - Serra dos Carajás, Folha SB.22-Z-A. Departamento Nacional da Produção Mineral e Companhia de Pesquisa e Recursos Minerais, Brasília, Brazil.

Holberg, O., 1987. Computational aspects of the choice of operator and sampling intervalfor numerical differentiation in lage-scale simulation of wave phenomena. Geophysical Prospecting, 35, 629–655.

Macambira, J. B., 2003. O ambiente deposicional da Formação Carajás e uma proposta de modelo evolutivo para a Bacia Grão Pará. Tese de Doutorado, Instituto de Geociências, Universidade Estadual de Campinas, São Paulo, Brazil, 217p.

Nogueira, P. V., 2014. Integração de sísmica de refração e eletrorresistividade para elaboração de um modelo 2D do deposito de ferro N4WS do complexo Serra Norte, Carajás-PA. Dissertação de Mestrado, Instituto de Geociências, Universidade de Brasília, Brasília, Brazil, 78p.

Reynolds, A. C., 1978. Boundary Conditions for the numerical solution of wave propagation problems. Geophysics, 43: 1099-1110.

Sandmeier, K. J. & Liebhardt, G., 1992. Software Refra. Geophysical Institut of Karlsruhe University, Germany.

Vasquez et al. (12 co-authors), 2008. Geologia e Recursos Minerais do Estado do Pará: Sistema de Informações Geográficas - SIG: Texto Explicativo dos Mapas Geológico e Tectônico e de Recursos Minerais do Estado do Pará, 1:1.000.000. CPRM, Belém, Brazil.

Zuchetti, M., 2007. Rochas máficas do supergrupo Grão Pará e sua correlação com a mineralização de ferro dos depósitos N4 e N5, Carajás, PA. Tese de Doutorado, UFMG, Minas Gerais, Brazil, 166p.